Received: 26 December 2025 | Revised: 15 April 2026 | Accepted: 16 April 2026

DOI: 10.1002/mp.70466

TECHNICAL NOTE

MEDICAL PHYSICS

Ion recombination correction in reference dosimetry for pencil beam scanned proton beams

Jun Ken Gan[1,2] | **Kah Seng Lew**[1,2] | **Clifford Ghee Ann Chua**[1,2] | **Calvin Wei Yang Koh**[2] | **Kang Hao Lee**[2] | **Masashi Yagi**[2,4] | **Wen Siang Lew**[1] | **James Cheow Lei Lee**[1,2] | **Sung Yong Park**[2,3] | **Hong Qi Tan**[1,2,3]

[1]Division of Physics and Applied Physics, School of Physical and Mathematical Science, Nanyang Technological University, Singapore, Singapore

[2]Division of Radiation Oncology, National Cancer Centre Singapore, Singapore, Singapore

[3]Duke-NUS Medical School, Singapore, Singapore

[4]Department of Radiation Oncology, The University of Osaka Graduate School of Medicine, Suita, Osaka, Japan

Correspondence
Tan Hong Qi,
Division of Radiation Oncology, National Cancer Centre Singapore, 30 Hospital Boulevard, 168583, Singapore.
Email: tan.hong.qi@nccs.com.sg

Abstract

Background: The 2024 IAEA TRS-398 revision updated recommendations for reference dosimetry and ion recombination corrections in pencil beam scanned (PBS) proton beams.

Purpose: This study evaluates the revised ion recombination methods for monoenergetic synchrotron-based PBS proton system across different energies, monitor units (MU), and ionization chamber types.

Methods: Reference-field measurements were performed using a synchrotron system at 70.2, 150.2, and 228.7 MeV and at 6, 50, and 200 MU. Charge-collection data were acquired using PTW Farmer and Advanced Markus chambers across 20–400 V. Ion recombination correction factors (k_s) were determined using the Jaffé plot extrapolation method and the TRS-398 two-voltage method (TVM) under different time structure assumptions. Charge multiplication in the chamber was addressed using both low voltage linear fitting and a semiempirical exponential model.

Results: For low energy, low MU fields, and TVM yielded k_s values within ~1% of the Jaffé extrapolation. For high-energy, high-MU fields, maximum differences of 6.25% (Farmer) and 1.62% (Advanced Markus) were observed. The synchrotron beam exhibited energy, MU, and chamber dependent time structure behavior, producing pulsed-like or continuous-like characteristics. Misclassification of the time structure resulted in additional k_s deviations of up to 2.49% (Farmer) and 0.59% (Advanced Markus). Charge multiplication was observed in the Advanced Markus chamber at voltages > 150 V. The exponential fitting successfully modeled this response and produced k_s values agreeing with low voltage fits within 1.5%, while avoiding subjective voltage cutoff selection.

Conclusion: The revised TRS-398 provides accurate ion recombination corrections for monoenergetic PBS fields at low energies and low MU. However, accuracy of ion recombination correction decreases at higher energies and MU, particularly when the time structure was ambiguous or chamber dependent. Charge multiplication in small volume chambers presents an additional source of uncertainty not fully addressed by TRS-398. Incorporating charge multiplication fitting methods may improve the robustness of reference dosimetry in synchrotron-based PBS proton therapy.

KEYWORDS
ion recombination, pencil beam scanned, reference dosimetry

1 | INTRODUCTION

In 2024, the International Atomic Energy Agency (IAEA) published a revision to the Technical Report Series 398 (TRS-398).[1] This revision was necessitated due to the advances in the medical physics field and the introduction and adoption of new radiotherapy technologies over the decades. The revision, amongst other additions, provides additional information on determining absorbed dose to water for pencil beam scanning (PBS) proton beams. This is part of a larger global trend of an increasing number of therapeutic ion beam clinics and with it an increasing need for a formal code of practice in dosimetry for PBS proton to reliably and accurately determine the absorbed dose to water. In the previous edition of TRS-398, the recommended configuration for proton beam reference dosimetry was the spread-out Bragg peak (SOBP). The revised TRS-398 now distinguishes between broad beam and PBS beam. For a PBS proton system, TRS-398 defines the reference condition for the determination of absorbed dose to water calibrated in a single energy pencil beam as using a single energy layer scanned field. As part of this revision, TRS-398 recommends the scanned field small ionization chamber setup for reference dosimetry of a PBS system. Additionally, the revised TRS-398 also formally provides additional guidance on ion recombination correction for proton beams. These additions extend TRS-398 and provides valuable guidance for clinics utilizing PBS delivery and particularly in synchrotron based therapeutic systems where the single energy layer configuration is more relevant in the dosimetry of a synchrotron beam.

TRS-398 recommends the use of gas filled ionization chambers as the dosimetry device of choice and list four influence factors that may result in an underestimation of the measured charge collected when using an ionization chamber: temperature, humidity, polarity and ion recombination. The focus of this study is on ion recombination, the process where free charges created during ionization events recombine to form a neutral particle before they can be collected at the electrodes, resulting in an underestimation of the measured charge collected and therefore lowered perceived dose delivered. For accurate dosimetry, the ion recombination of the chamber must be known and corrected for; this is the ion recombination correction factor, k_s. There are 2 main types of recombination; initial and volume recombination.[2–4] Initial recombination is dependent on the linear energy transfer (LET) of the of the beam and TRS-398 recommends that for heavy ion beams, initial recombination may be nontrivial and should be considered during recombination corrections. Volume recombination is dependent on the time structure of the beam and is split into two distinct regimes: pulsed beams and continuous beams.[5] A beam is categorized as a pulsed beam if the time between pulses is larger than the chamber's charge collection time, and the charge collection time is larger than the pulse duration.[5,6] Otherwise, the beam should be considered as a continuous beam for the purpose of ion recombination. From Boag's model, the volume recombination contribution for a pulsed beam is dependent on the inverse of the first power of the bias voltage, $1/V$ while for a continuous beam, it is dependent on the inverse of the second power of bias voltage, $1/V^2$.[5] In the case where volume recombination is the dominating contribution to the overall k_s compared to the initial recombination, it can be approximated that k_s of pulsed beams are linearly dependent on the $1/V$ and $1/V^2$ for continuous beams.[7] This forms the basis of modern ion recombination correction factor calculations method like the widely used two-voltage method (TVM).[8]

In ion recombination, the time structure of a beam is important as there are differences in the dosimetry calculation of a pulsed and continuous beam when applying Boag's model [5]. While cyclotron and slow extraction synchrotrons are inherently pulsed due to the radiofrequency (RF) acceleration, the short pulse repetition times in modern machines was used to justify the continuous beam nature with regards to ion recombination.[1,9–11] However, these classifications are ultimately an empirical recommendation and users should still conduct their own verification to determine the behavior and time structure of their beam.

Despite the new additions to the revised TRS-398, gaps remain regarding its recommendations for ion recombination. Firstly, due to the fundamental differences in how k_s is calculated in pulsed versus continuous beams, any ambiguity in the beam's time structure will result in dosimetry error. In synchrotron beams, the time structure is nontrivial and varies based on factors such as energy level and monitor unit (MU) per spot.[12] Consequently, if users follow TRS-398 recommendations and incorrectly assume a continuous time structure for what is effectively a pulsed beam, significant dosimetry errors may occur. Secondly, TRS-398 lacks strong recommendations for addressing charge multiplication effects in reference ionization chambers. The current protocol advises that charge collection be conducted within an operational voltage range where the chamber response is linear—this condition is necessary for using the Jaffé plot method to determine saturation charge and k_s. However, it has been demonstrated that charge multiplication can occur even within the recommended operating range of the chamber.[13–16] Such cases are currently not addressed by TRS-398, leaving users without a validated correction method.

This study evaluates the implementation of the revised TRS-398 protocol for determining k_s within the context of our clinic's Hitachi Probeat synchrotron system using the reference conditions for a monoenergetic scanned proton beams. A parallel plate Advanced

Markus chamber and a cylindrical Farmer chamber were studied to represent two different geometries of ionization chambers. While the protocol provides a framework for monoenergetic scanned beams, the unique time structure of a synchrotron beam presents nontrivial challenges, as delivery timing varies with energy, dose (MU), and chamber geometry. Additionally, the study will also apply two proposed methods for addressing charge multiplication in the advanced Markus chamber that are currently not provided within TRS-398. Lastly, the TVM following TRS-398 protocol and the Jaffé plot extrapolation method are compared to evaluate the level of confidence and accuracy of the k_s value in a synchrotron proton therapy system.

2 | METHODS

2.1 | Overview of irradiation condition and experimental measurements

The study was conducted using a Hitachi Probeat PBS proton system. A monoenergetic scanned field consisting of a spot spacing of 2.5 mm with a total spot number of 1681 spots across the 10×10 cm^2 field size was used for this study. This follows the reference condition for PBS delivery system as stated in TRS-398.[1] A total of 3 different energy layers (70.2 MeV, 150.2 MeV, 228.7 MeV) and 3 different monitor units (MU) (6 MU, 50 MU, 200 MU) were investigated. The energy choice corresponded to the lowest and highest energy level available. The MU was chosen to span a practical range corresponding to the minimum MU per spot and close to the maximum MU per spot.[17,18] The MU per spot affects the average spot dwell time spot in PBS and the combination of different energy and MU gives a good representation of the different irradiation conditions and time structure in a proton PBS irradiation. For each permutation, the charge-collection measurement was repeated three to seven times to achieve a coefficient of variation below 1%. Two chambers were investigated in this study, PTW 30013 Farmer chamber (PTW Freiburg GmbH, Freiburg, Germany) and PTW 34045 Advanced Markus chamber (PTW Freiburg GmbH, Freiburg, Germany). [19] The same chambers were used throughout the experiment for consistency and the chambers were operated at a range of bias voltages between 20 and 400 V. The chambers measured were connected to and measured with the same PTW UNIDOSE [webline] electrometer (PTW Freiburg GmbH, Freiburg, Germany). The chambers were placed at 2.0 cm water equivalent depth within chamber specific holders and aligned to the isocenter to measure the dose at the plateau region of the depth-dose curve.

k_s was calculated according to the ion recombination correction methods provided by TRS-398 for proton beams and both the Jaffé plot extrapolation method and TVM were investigated in this study. Due to the presence of charge multiplication in the Advanced Markus chamber, two charge multiplication correction methods were evaluated alongside the linear extrapolation method with Jaffé plot. The values of pulsed, pulsed-scanned and continuous beams k_s were determined using TRS-398′s TVM and compared against the ground truth value obtained using the Jaffé plot extrapolation method for different integer voltages ratios. The percentage difference from the ground truth was calculated as a means of determining the error that could arise from choosing the wrong beam time structure and the uncertainty from the different methods of calculating k_s.

2.2 | Jaffé plot extrapolation method

An empirical method for determining the beam time structure and k_s is the use of Jaffé plots as recommended in TRS-398.[1] First a chamber is irradiated at a range of bias voltages (V) up to the manufacturer's maximum voltage and the corresponding charge collected recorded as the measured charge (M). Next, the plots of $1/M$ against $1/V$ and $1/V^2$ are compared. For a beam with pulsed time structure, the inverse of the chamber response, $1/M$, would vary linearly with $1/V$ while a beam with a continuous time structure should show a linear dependency in the $1/V^2$ plot. It should be noted that this method assumes that volume recombination is the dominant contribution to ion recombination.

In this study, the plots of $1/M$ against $1/V$ and $1/M$ against $1/V^2$ were created and compared to determine the time structure of the beam. A weighted linear regression was fitted to both plots and the coefficient of fit, R^2, were compared to determine the line of best fit. The weights of the linear regressions were determined from the standard deviation of the repeated measurement of the charge. Bootstrapping was used to determine the expected standard deviation of the R^2 values as a confidence interval of the goodness of fits. In the cases where the bootstrapped intervals overlapped, the time structure was indeterminate and could not be reliably determined using the TRS-398 Jaffé plot method and fit with the highest nominal R^2 was selected. If the R^2 in the plot of $1/M$ against $1/V$ is higher with no overlap in the bootstrapped intervals, the beam is taken to be a pulsed beam and vice versa. After determining the time structure of the beam, the ion recombination factor at any bias voltage can be determined using the Jaffé plot extrapolation method. From the best linear fit case (pulsed or continuous), the ordinate intercept (where $V \to \infty$) was determined from the fitting coefficients and this value is therefore the inverse of the saturation charge, $1/M_{sat}$. The saturation charge is a theoretical point of perfect charge separation and collection without charge recombination effects. The value of the saturation charge can be subsequently used to

calculate the value of k_s using the measured charge, $M_{measured}$, at any arbitrary voltage:

$$k_s = \frac{1}{f} = \frac{M_{sat}}{M_{measured}}. \quad (1)$$

In this study, the value of k_s determined from Equation (1) using the extrapolation method will be referred to as the ground truth value and would be the basis of comparison with the other methods in this study.

2.3 | Overview of TVM

If the time structure of the beam is known, TRS-398 recommends the use of the TVM to determine k_s. This method uses the response of the chamber at two different voltages to determine the ion recombination correction factor. The main benefit of TVM is that by choosing the appropriate pair of voltages, the ion recombination correction factor can be easily determined. In using TVM, it is assumed that the response of the chamber is linear within the range of the pair of chosen voltages used and that volume recombination is the dominant recombination event occurring. Additionally, it is recommended that the ratio of the chosen bias voltage is larger than 3.

As recommended by TRS-398, the k_s for a pulsed, pulsed scanned and continuous proton beam can be determined using the TVM as follows[1],

$$k_{s,\ pulsed\ and\ pulsed\ scanned} = a_0 + a_1\left(\frac{M_1}{M_2}\right) + a_2\left(\frac{M_1}{M_2}\right)^2, \quad (2)$$

and

$$k_{s,\ continuous} = \frac{\left(\frac{V_1}{V_2}\right)^2 - 1}{\left(\frac{V_1}{V_2}\right)^2 - \frac{M_1}{M_2}}. \quad (3)$$

Equation (2) applies to both pulsed beams and pulsed scanned beams while Equation (3) applies to only continuous beams. The variables a_n are quadratic fit coefficients numerically determined by Weinhous and Meli and provided in TRS-398.[1,20] M_1 and M_2 are the chamber response at the two voltages investigated, corresponding to the two voltages V_1 and V_2. Where V_1 is the operating voltage of the chamber and V_2 is a lower voltage within the linear region. The use of Equations (2) and (3) assumes a linear relationship between the response in $1/V$ and $1/V^2$ respectively for the $[V_2,\ V_1]$ voltage intervals. The actual relationship can also be highly nonlinear in the presence of charge multiplications in small ionization chamber. Hence, the only way to verify the linear region of the chamber is to therefore empirically determine it through irradiating a series of bias voltages in a Jaffé plot. In this study, the k_s under all three possible time structures were determined using the TVM methods. The percentage difference from the ground truth value was calculated to determine the error that could arise from choosing the wrong beam time structure.

2.4 | Charge multiplication corrections

One issue that complicates dosimetry using ion chambers is the presence of charge multiplication. Charge multiplication occurs when the charges are overaccelerated with sufficient energy to cause secondary ionization and while there is no exact point where dielectric breakdown of air occurs, it has been reported that for air filled ionization chambers, charge multiplication occurs around 150 to 200 V/mm.[13,14,21] It has been demonstrated that the application of the TVM in the presence of charge multiplication can result in an overestimation of k_s.[13] In addition, charge multiplication may occur even when operated within the manufacturer's recommended voltages. Thus, for detectors that demonstrates charge multiplication effects at higher voltages, a low bias voltage range fit should be used to obtain a more accurate saturation charge and estimation of the ion recombination.[13–16]

Alternatively, it has also been demonstrated that the use of a semiempirical exponential term as part of the Jaffé plot fitting could result in a good fitting in the presence of charge multiplication.[14,22,23] This exponential term was first proposed by Zankowski et al for continuous beams Equation (4)[14] and by DeBlois et al for pulsed beams Equation (5)[22],

$$\frac{1}{Q} = \left[\frac{1}{Q_{sat}} + \frac{\alpha}{V} + \frac{\beta}{V^2}\right] e^{-\gamma V}, \quad (4)$$

and

$$\frac{1}{I} \approx \left[\frac{1}{I_{sat}} + \frac{\lambda_p}{V}\right] e^{-\gamma V}. \quad (5)$$

The variables of $\alpha,\ \beta,\ \lambda_p$ and γ were treated as fitting parameters and a custom fitting function was created. Using this fitting, the saturation charge was determined from the fitting parameters.

Both methods of accounting for charge multiplication (low voltage linear fit and exponential fit) will be applied, as necessary, to chambers exhibiting charge multiplication in this study. In the absence of charge multiplication, the Jaffé plot should remain linear across the range of voltages tested and the presence of charge multiplication will result in the plot deviating from linearity. This

deviation from linearity was determined visually from the plot and the range of voltages before the onset of charge multiplication were used as the low voltage fitting range. The saturation charge obtained using these two methods will be treated as the ground truth value and TVM will be compared against it.

3 | RESULTS

3.1 | Jaffé plot and fitting results for Farmer and advanced Markus chambers

The response of the two chambers was examined across a range of bias voltage, from 20 to 400 V. The Jaffé plots were normalized using an absolute maximum scaling normalization to ensure a consistent scale for visualization. The normalized Jaffé plot and low voltage linear fits of the charge collected using the Farmer and Advanced Markus chamber are shown in Figure 1 and Figure 2 respectively. The Farmer chamber did not exhibit any noticeable charge multiplication and the full range of bias voltages were used for subsequent analysis for regression analysis. From Figure 2, the Advanced Markus chamber exhibits strong charge multiplication effects at bias voltages above 150 V. This is evident from the nonlinear shoulder leading to a sharp decline in $1/M$ from linearity at small $1/V$ and $1/V^2$ values. Following the recommendations of[13, 16], a low bias voltage range of 0 to 150 V was used to determine the saturation charge according to the Jaffé plot extrapolation method. Due to the presence of charge multiplication in the Advanced Markus chamber, an additional fit using the semiempirical exponential term was attempted for the Advanced Markus dataset. The normalized fit using the semiempirical exponential term for the Advanced Markus chamber is shown in Figure 3. The error bars in the Jaffé plots represent one standard deviation of the inverse charge collected. Additionally, the Farmer chamber demonstrated a very stable response within its operational voltage range, while the Advanced Markus chamber demonstrated significantly more fluctuations and variance in the measured charge.

The R^2 of the weighted linear regression on the Jaffé plots are shown in Table 1 and Table 2 for the Farmer and Advanced Markus (low voltage linear fit) chambers respectively. The uncertainty in the R^2 values was calculated using the bootstrap method as an indicator of the confidence in the fit. The final best fit plot used to determine the M_{sat} was determined by comparing the R^2 in $1/V$ against $1/V^2$ and choosing the fit of the higher R^2. From Table 1, the results of the Farmer chamber showed a mixture of pulsed and continuous time structure. A closer look at the R^2 values suggests that most irradiation conditions favoured a continuous time structure in the Farmer chamber. Additionally, the time structure was more pulsed at low energy and low MU and more continuous at high energy and high MU in the Farmer chamber. From the R^2 values for the Advanced Markus chamber fit in Table 2, the time structure appears to be indeterminate, where the goodness of fit in both $1/V$ and $1/V^2$ were similar and it was not feasible to conclusively determine the time structure based on the R^2 values. Due to the charge multiplication effect in the Advanced Markus chamber for voltages above 150 V, an additional fit using Equation (4) and Equation (5) was conducted and shown in Figure 3 and Table 3. From Figure 3, the response of the chamber at voltages within the charge multiplication region was well fitted with the addition of the proposed semiempirical exponential term. However, similar to the linear fit for Advanced Markcus chamber, the comparison of the R^2 values showed an indeterminate time structure.

3.2 | Comparison of TVM with the ground truth k_s from Jaffé plot

The TVM was applied to the dataset and the k_s values were computed at different integer voltage ratios and for the three different time structure as provided in TRS-398. The k_s obtained using TVM was compared to the ground truth value determined from the Jaffé plot linear extrapolation method and exponential fit method. Subsequently, the percentage difference was calculated to demonstrate the potential error that could arise from the application of TVM. The percentage difference of Farmer and Advanced Markus chamber are shown in Figure 4 and Figure 5 respectively when considering only the linear fit method to calculate the k_s. Figure 6 shows the percentage difference when using the modified ion recombination equation with the charge multiplication exponential term to calculate M_{sat} and k_s. The error bars shown were derived from propagating the errors of the charge measurement and the statistical fitting. The percentage difference of TVM for both pulsed and continuous time structure compared to ground truth were not significantly different from 1% of the ground truth and the error bars generally coincided with $\pm$1% of the ground truth. Higher energy and higher MU tended to show larger uncertainty in the calculated k_s when using TVM.

From Figure 4, the highest error observed for the Farmer chamber was 6.25% at 228.7 MeV – 200 MU for continuous time structure, and the largest percentage difference between the various TVM observed was 2.49% between pulsed and continuous time structure at 228.7 MeV – 200 MU for a voltage ratio of 3.

From Figure 5, the highest error observed for the Advanced Markus chamber was 1.62% at 228.7 MeV – 50 MU pulsed scanned time structure, and the largest percentage difference between the various TVM observed was 0.59% between pulsed-scanned and con-

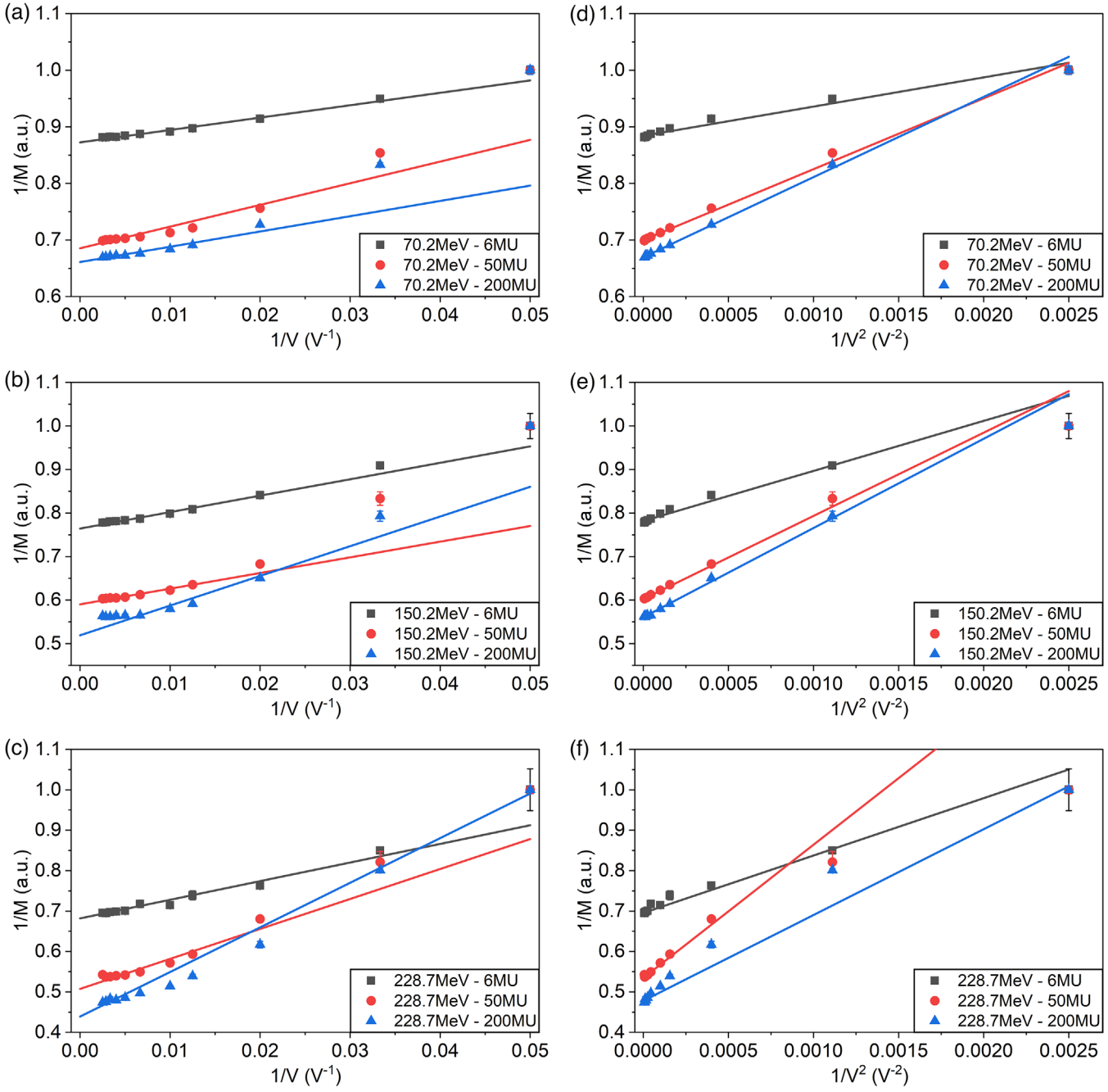

FIGURE 1 Normalised Jaffé plot of Farmer chamber. No noticeable charge multiplication was observed when measuring with the Farmer chamber. The response of the Farmer chamber was more stable with smaller variance in the charge collected. Saturation charge was determined from the ordinate intercept.

tinuous time structure at 228.7 MeV – 50 MU at a voltage ratio of 3.

From Figure 6, when applying the charge multiplication exponential term for Advanced Markus chamber, the highest error observed was reduced to 2.83% at 228.7 MeV – 50 MU continuous time structure, and the largest percentage difference observed between TVM was 0.60% between pulsed and continuous time structure at 228.7 MeV – 50 MU for a voltage ratio of 3.

4 | DISCUSSION

This study investigates the ion recombination correction factor under reference condition for monoenergetic pencil beam scanning proton. The result of this study shows that application of TRS-398 reference condition and ion recombination methods following TVM results in an acceptable estimate of the ion recombination for most irradiation conditions except for high energy and high

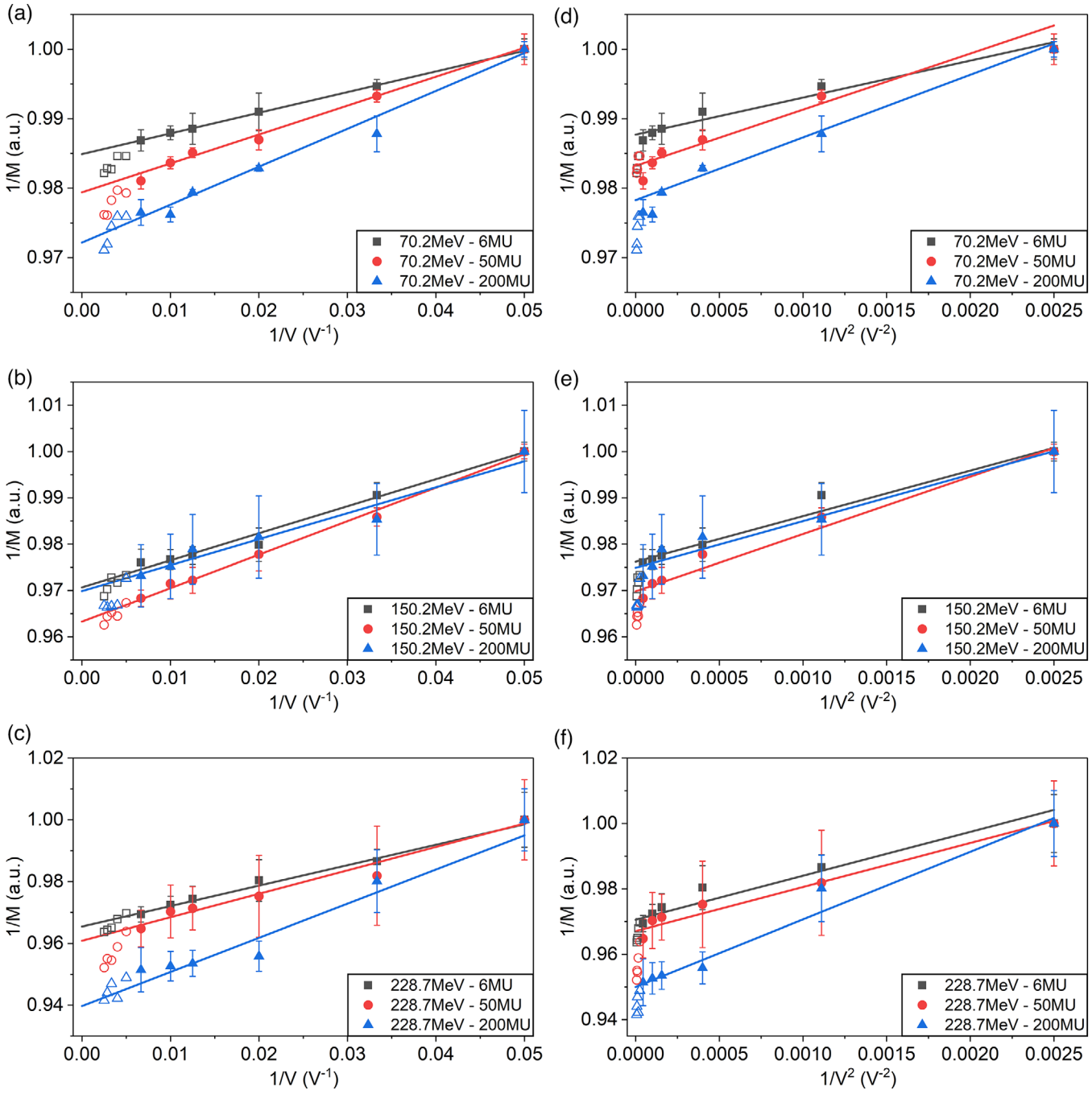

FIGURE 2 Normalised Jaffé plot of Advanced Markus chamber and low voltage fit. Solid points were the data points used in the linear fitting. Hollow points were measurements exhibiting charge multiplication and excluded from the fit. Charge multiplication was evident at voltages above 150 V. Charge measurements using the advanced Markus chamber demonstrated large variance in the charge collected. Saturation charge was determined from the ordinate intercept of the line in the figure.

MU fields. Overall, the TVM value differed from the Jaffé plot method within 1% (Figure 4 and Figure 5). At high energy and MU, errors of up to 6.25% and 1.62% from ground truth were observed in Farmer and Advanced Markus chambers respectively. The method of comparing Jaffé plots of $1/V$ and $1/V^2$ showed that the time structure is dependent on the energy and MU of the irradiation conditions, as shown in Table 1. From our results, misidentifying the time structure and applying the wrong TVM method to calculate k_s could lead up to a 2.49% and 0.59% error when using the Farmer chamber and Advanced Markus chamber respectively.

Additionally, in this study we also investigated a proposed method for addressing charge multiplication in

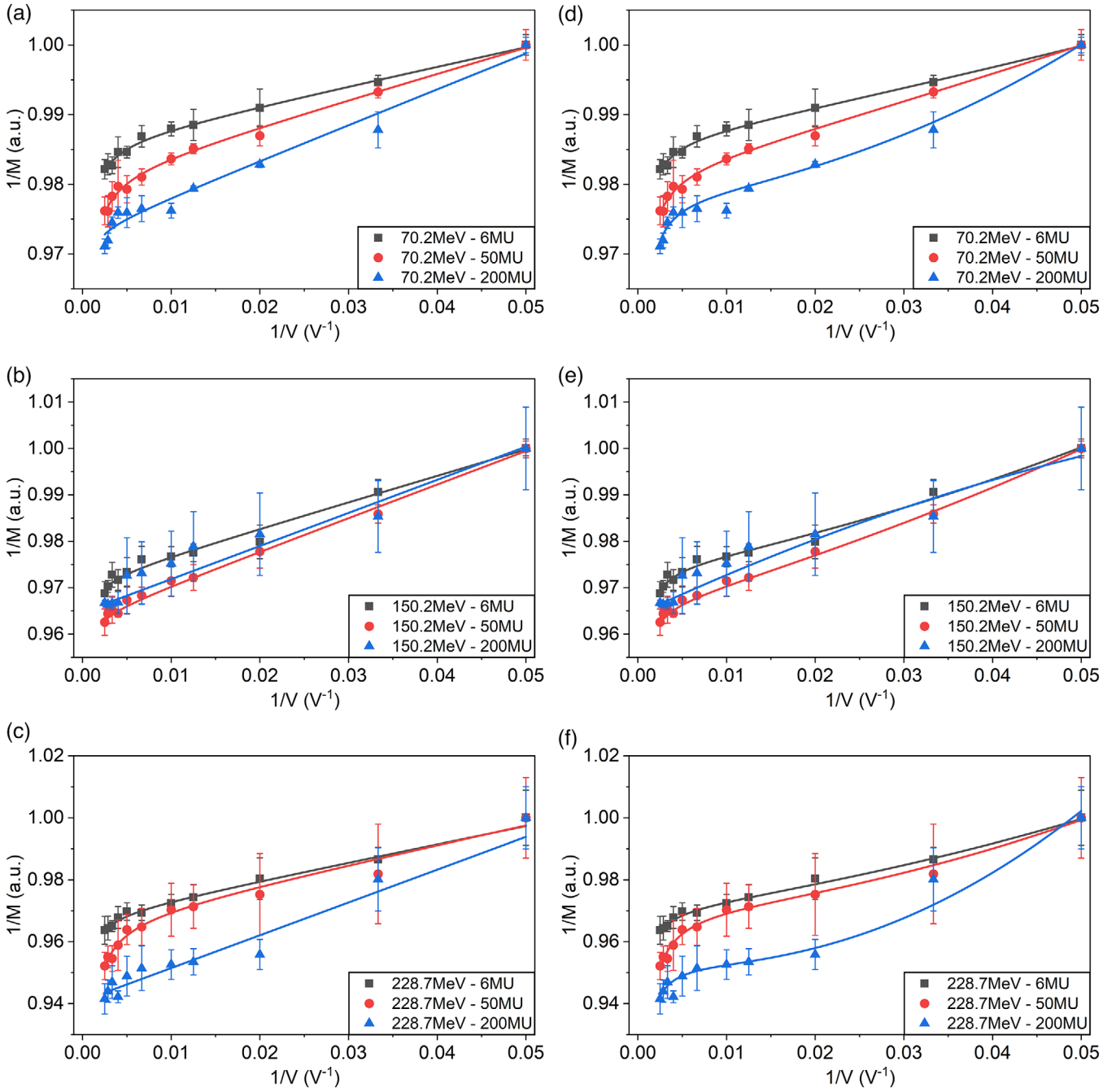

FIGURE 3 Normalised Jaffé plot of advanced Markus chamber using the semiempirical exponential fit. Figures 3A–3C were fitted using Equation (5) and 3D–3F were fitted using Equation (4). The addition of the exponential term was able to address the response of the chamber in the charge multiplication regime above 150 V. The saturation charge was determined from the fitting coefficients obtained.

the chamber by introducing an exponential term. This method appears to be promising and was able to fit the charge response within the charge multiplication region. Table 4 shows the k_s calculated from both the TRS linear fit and the proposed exponential fit. The k_s values obtained using the exponential fit were comparable to those derived from the low voltage range linear fit method, with differences of less than 1.5%. However, the primary advantage of the exponential fit over the low voltage range linear fitting method is that the exponential fit eliminates the guesswork involved in selecting the cutoff voltage for the charge multiplication region, which is required when using the linear fit approach.

While TRS-398 recommends categorizing slow extraction synchrotrons as continuous beams for the purpose of ion recombination, an assessment using TRS-398 recommendations showed that the time structure may vary between pulsed and continuous

TABLE 1 R^2 of linear fits for Farmer chamber. While the time structure appears to be a mix of both pulsed and continuous, the higher R^2 in $1/V^2$ suggests a more continuous time structure when measuring with the Farmer chamber. The uncertainty in R^2 was obtained via bootstrapping and it represents one standard deviation.

	R^2 in $1/V$	R^2 in $1/V^2$	Time structure
70.2MeV - 6MU	0.967 ± 0.003	0.908 ± 0.005	Pulsed
70.2MeV - 50MU	0.793 ± 0.002	0.995 ± 0.001	Continuous
70.2MeV - 200MU	0.796 ± 0.004	0.996 ± 0.002	Continuous
150.2MeV - 6MU	0.948 ± 0.001	0.938 ± 0.003	Pulsed
150.2MeV - 50MU	0.718 ± 0.007	0.985 ± 0.013	Continuous
150.2MeV - 200MU	0.930 ± 0.005	0.975 ± 0.004	Continuous
228.7MeV - 6MU	0.964 ± 0.006	0.983 ± 0.006	Continuous
228.7MeV - 50MU	0.884 ± 0.009	0.955 ± 0.028	Continuous
228.7MeV - 200MU	0.992 ± 0.003	0.991 ± 0.004	Indeterminate

TABLE 2 R^2 of linear fit for advanced Markus chamber. While the fits favour a pulsed time structure, the coefficients between $1/V$ and $1/V^2$ fits were very similar and it may be difficult to differentiate the time structure especially in the presence of outliers or erroneous charge collection. The uncertainty in R^2 was obtained via bootstrapping and it represents one standard deviation.

	R^2 in $1/V$	R^2 in $1/V^2$	Time structure
70.2MeV - 6MU	0.999 ± 0.073	0.965 ± 0.090	Indeterminate
70.2MeV - 50MU	0.987 ± 0.023	0.929 ± 0.048	Pulsed
70.2MeV - 200MU	0.988 ± 0.037	0.954 ± 0.023	Indeterminate
150.2MeV - 6MU	0.992 ± 0.055	0.981 ± 0.052	Indeterminate
150.2MeV - 50MU	0.996 ± 0.034	0.983 ± 0.041	Indeterminate
150.2MeV - 200MU	0.956 ± 0.226	0.955 ± 0.232	Indeterminate
228.7MeV - 6MU	0.991 ± 0.133	0.939 ± 0.172	Indeterminate
228.7MeV - 50MU	0.972 ± 0.250	0.935 ± 0.252	Indeterminate
228.7MeV - 200MU	0.906 ± 0.087	0.969 ± 0.099	Indeterminate

TABLE 3 R^2 of the exponential fits for advanced Markus chamber to account for charge multiplication effect. R^2 in pulsed was obtained by fitting with Equation (5) while R^2 in continuous was obtained by fitting with Equation (4). The uncertainty in R^2 was obtained via bootstrapping and it represents one standard deviation.

	R^2 in pulsed	R^2 in continuous	Time structure
70.2MeV - 6MU	0.994 ± 0.020	0.994 ± 0.022	Indeterminate
70.2MeV - 50MU	0.994 ± 0.018	0.994 ± 0.018	Indeterminate
70.2MeV - 200MU	0.978 ± 0.007	0.991 ± 0.008	Pulsed
150.2MeV - 6MU	0.992 ± 0.016	0.993 ± 0.017	Indeterminate
150.2MeV - 50MU	0.996 ± 0.011	0.997 ± 0.012	Indeterminate
150.2MeV - 200MU	0.921 ± 0.110	0.927 ± 0.116	Indeterminate
228.7MeV - 6MU	0.985 ± 0.074	0.987 ± 0.081	Indeterminate
228.7MeV - 50MU	0.974 ± 0.136	0.977 ± 0.139	Indeterminate
228.7MeV - 200MU	0.927 ± 0.047	0.976 ± 0.048	Continuous

depending on the chamber ion collection time and both the energy and MU of the field. From Table 1, we observe a pulse like time structure in the Farmer chamber at low energy and MU and a continuous time structure at high energy and high MU. This observation can be explained by the increase in individual spot dwell time at higher MUs, which may cause the ionization chamber to perceive the beam as continuous during irradiation. From Table 2, we observe a pulsed time structure for the Advanced Markus chamber. From our

TABLE 4 Ion recombination correction factor in advanced Markus chamber as calculated using a low voltage linear fit and using the proposed exponential fit. The actual values of k_s obtained using both methods were similar. The advantage of the exponential fit is in its ability to fit the response within the charge multiplication region; hence the user does not need to determine a cut off voltage for the fit.

	k_s from low voltage linear fit	k_s from exponential fit	Percentage difference from low voltage linear fit%
70.2MeV - 6MU	0.998 ± 0.002	0.997 ± 0.002	0.14
70.2MeV - 50MU	0.999 ± 0.003	0.997 ± 0.003	0.22
70.2MeV - 200MU	1.002 ± 0.001	0.995 ± 0.001	0.72
150.2MeV - 6MU	1.002 ± 0.008	0.998 ± 0.009	0.41
150.2MeV - 50MU	1.002 ± 0.004	0.999 ± 0.006	0.27
150.2MeV - 200MU	0.998 ± 0.002	1.002 ± 0.003	−0.40
228.7MeV - 6MU	0.999 ± 0.028	0.994 ± 0.092	0.57
228.7MeV - 50MU	0.994 ± 0.011	0.982 ± 0.006	1.18
228.7MeV - 200MU	1.001 ± 0.007	0.989 ± 0.012	1.21

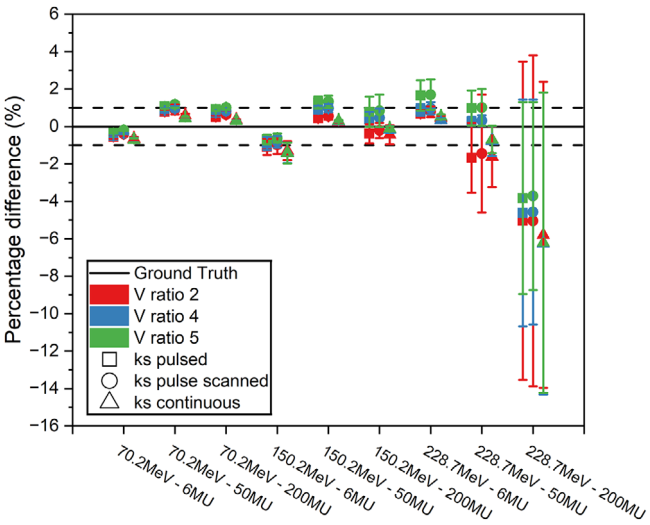

FIGURE 4 Percentage difference of the two-voltage method from ground truth value for Farmer chamber. Error bars were calculated via error propagation of the standard deviation of the charge collected and the statistical fitting. The dotted lines represent the 1% threshold and percentage difference was generally within 1% with higher energy and MU fields showing larger error. In general, the average k_s value lies within the 1% tolerance with the 228.7 MeV and 200, 50 MU fields showing the largest error.

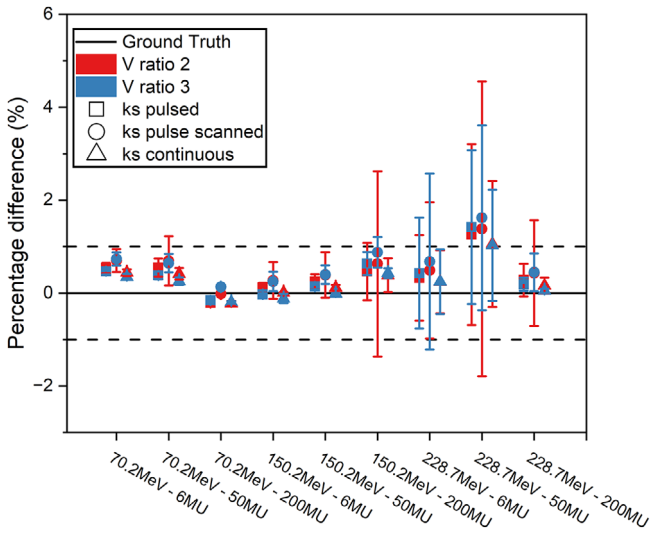

FIGURE 5 Percentage difference of the TVM from ground truth value for Advanced Markus chamber using the low voltage linear fits. Error bars were calculated via error propagation of the standard deviation of the charge collected and the statistical fitting. The dotted lines represent the 1% threshold and percentage difference was generally within 1% with higher energy and MU fields showing larger error. In general, the average k_s value lies within the 1% tolerance except the measurement at 228.7 MeV and 50 MU.

results the time structure was predominantly pulse-like when measured using the Advanced Markus chamber and continuous-like when measured using the Farmer chamber. This could be attributed to the difference in ion collection time of the chambers. The Advanced Markus chamber has a collection time of 22 μs compared to 140 μs for Farmer chamber at their operational voltages of 300 and 400 V respectively.[19] Following the Boag model of volume recombination, the shorter ion collection time of the Advanced Markus chamber might be sufficient at resolving parts of the pulse structure in the beam, resulting in the pulsed time structure observed in our study.[5] This observation is of interest as our results contradicts the recommendations of TRS-398 of treating slow extraction synchrotron beams as continuous beams for the purpose of ion recombination. As shown in this study, this miscategorising of the time structure when using different chambers could result in error especially in a Farmer chamber. While the radio frequency acceleration signal inherently creates a pulsed time structure within the synchrotron ring, it has been reported that the slow extraction process can lead to significant distortion and the loss of the distinct pulse time structure, additionally the time structure of the beam may vary with different irradiation conditions.[24,25] Therefore, in the case of slow extraction

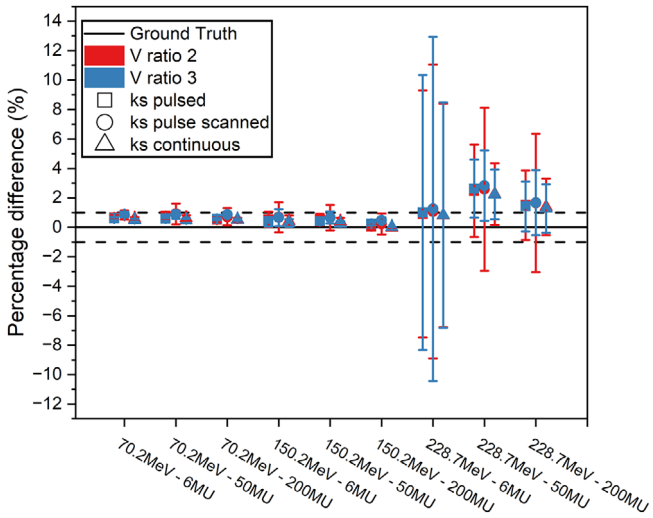

FIGURE 6 Percentage difference of the TVM from ground truth value for Advanced Markus chamber using the exponential fitting. Error bars were calculated via error propagation of the standard deviation of the charge collected and the statistical fitting. Ground truth was determined using the saturation charge obtained using Equations (4) and (5). The dotted lines represent the 1% threshold and percentage difference was generally within 1% with higher energy and MU fields showing larger error. In general, the average k_s value lies within the 1% tolerance except the measurement at 228.7 MeV. The percentage differences were rather similar to the results from the use of low voltage linear fit across a lower voltage region and could be a viable method for addressing chambers with charge multiplication within its operating voltages range.

synchrotron beams, it might be recommended to adopt a more empirical approach to ion recombination time structure instead of the current prescribed continuous time structure.

During measurements, large variations of up to 5% as indicated by the error bars in Figure 2 and Figure 3 was observed in the charge collected when measuring with the chambers. Additionally, the Advanced Markus measurements showed stochastic fluctuations that deviated from the expected saturation curve despite the low coefficient of variance and repeated readings. It is believed that these errors were due to spot position deviations within a spill that had a relatively larger dosimetric effect on small sensitive volume chamber like the Advanced Markus chamber compared to the Farmer chamber which has a larger sensitive volume. This problem was further accentuated for high energy proton where the smaller spot size combined with dispersion and spill change effects would result in larger type A uncertainty during repeated dosimetric measurement.[17, 26] This also results in the larger error bars in Figures 4–6 for higher proton energies. This study highlights the challenge of establishing the time structure for the dosimetry using the Jaffé plot when the dosimetry measurements were plagued with high error bars resulting from spot position errors. This was the main reason why most of the comparison in Tables 2 and 3 lead to an indeterminate result.

There are some limitations in this study. Firstly, for measurements conducted at the 70.2 MeV layer, the set-up condition does not follow TRS-398 relative dosimetry conditions. The measurement was conducted at 2 cm plastic water depth while TRS-398 recommendations would require the 70.2 MeV layer to be measured at 1 cm plastic water depth. This deviation from TRS-398 reference condition was chosen to facilitate the comparison of data between energy levels. This would be an important consideration for accurate dosimetry during TPS commissioning for example, however, in our study the measurements were still conducted in the plateau region and it should not affect the results of the current recombination study. Secondly, the experiment uses plastic water phantoms in lieu of water as the reference medium, while TRS-398 discourages the use of plastic water phantom for proton beams for reference dosimetry as their water to plastic fluence correction factors are not well known. However, as this experiment is focused on the relative differences, the use of plastic water should not have any significant impact on the accuracy of our results. Third, the study did not evaluate the use of the generalized approach by De Almeida and Niatel as recommended in TRS 398.[1, 27, 28] While this method would address some of the issue regarding indiscriminate time structure, it does not address the issue of charge multiplication effects in small ionization chambers that is not sufficiently covered by TRS 398. Lastly, our study was conducted using only two detectors and using one machine and our results might not be entirely representative of all possible conditions. Future studies using additional detectors and other slow extraction synchrotron machines would provide a more comprehensive view on ion recombination for PBS synchrotron beams.

5 | CONCLUSION

In this study, we demonstrated the use of TRS-398 reference dosimetry condition for monoenergetic pencil beam scanned proton beams in a Hitachi Probeat system for determining ion recombination correction factor. Our results showed that the reference conditions and methods of TRS-398 are sufficiently accurate for determining k_s, TVM was generally within 1% of Jaffé plot extrapolation method for low energy and low MU fields. However, reliability and accuracy decreased with increasing energy and MU. Using the methods of TRS-398, establishing the time structure of a slow extraction synchrotron beam was nontrivial and both pulsed and continuous time structure was observed in our study. This ambiguity in the time structure could result in a difference in the k_s of up to 2.49% when using a Farmer chamber and 0.59% for Advanced Markus chamber.

Lastly, there is currently a lack of information on how to correct for charge multiplication in ionization chambers at operating voltage range. In this study, we attempted two proposed methods for addressing charge multiplication and demonstrated that the use of these methods could result in a fairly accurate k_s and could be a viable method for addressing charge multiplication in chambers.

ACKNOWLEDGMENTS

The authors have nothing to report.

CONFLICT OF INTEREST STATEMENT

The authors declare no conflicts of interest.

FUNDING INFORMATION

Hong Qi Tan is supported by the Duke-NUS Oncology Academic Program Goh Foundation Proton Research Programme (08/FY2023/EX(SL)/163-A218(b)), Clinical & Systems Innovation Support – Innovation Seed Grant (08/FY2022/P2/02-A68)

ORCID

Jun Ken Gan https://orcid.org/0009-0000-5695-1540
Clifford Ghee Ann Chua
https://orcid.org/0000-0002-6887-7015
Calvin Wei Yang Koh
https://orcid.org/0000-0002-6434-2400
Kang Hao Lee
https://orcid.org/0000-0002-1824-2724
Masashi Yagi
https://orcid.org/0000-0002-2827-5407
Wen Siang Lew
https://orcid.org/0000-0002-5161-741X
Sung Yong Park
https://orcid.org/0000-0002-7961-2119
Hong Qi Tan https://orcid.org/0000-0001-7878-4544

REFERENCES

1. IAEA 2024 TRS-398 Absorbed Dose Determination in External Beam Radiotherapy Revision 1 (International Atomic Energy Agency)
2. Jaffé G. Zur theorie der ionisation in kolonnen. *Annalen Der Physik*. 1913;347:303-344. doi:10.1002/andp.19133471205
3. Mie G. Der elektrische strom in ionisierter luft in einem ebenen kondensator. *Annalen Der Physik*. 1904;318:857-889. doi:10.1002/andp.18943180502
4. Boag JW, Wilson T. The saturation curve at high ionization intensity Br. *J Appl Phys*. 1952;3:222.
5. Boag JW. 3 - Ionization Chambers. *The Dosimetry of Ionizing Radiation* ed Kase KR, Bjärngard BE and Attix FH, Academic Press 1987:169-243.
6. Boag JW. Ionization measurements at very high intensities. Pulsed radiation beams. *Br J Radiol*. 1950;23:601-611. doi:10.1259/0007-1285-23-274-601
7. Rossomme S, Horn J, Brons S, et al. Ion recombination correction factor in scanned light-ion beams for absolute dose measurement using plane-parallel ionisation chambers. *Phys Med Biol*. 2017;62(13):5365-5382.
8. Boag JW, Currant J. Current collection and ionic recombination in small cylindrical ionization chambers exposed to pulsed radiation. *Br J Radiol*. 1980;53:471-478. doi:10.1259/0007-1285-53-629-471
9. Rossomme S, Delor A, Lorentini S, et al. Three-voltage linear method to determine ion recombination in proton and light-ion beams. *Phys Med Biol*. 2020;65:045015. doi:10.1088/1361-6560/ab3779
10. Palmans H, Thomas R, Kacperek A. Ion recombination correction in the Clatterbridge Centre of Oncology clinical proton beam. *Phys Med Biol*. 2006;51:903-917. doi:10.1088/0031-9155/51/4/010
11. Rossomme S, Hopfgartner J, Lee ND, et al. Ion recombination correction in carbon ion beams. *Med Phys*. 2016;43:4198-4208. doi:10.1118/1.4953637
12. Chua CGA, Furutani KM, Lee KH, et al. A comprehensive characterization of the temporal characteristics of dose driven continuous scanning in proton therapy. *Phys Med Biol*. 2025;70:145003. doi:10.1088/1361-6560/ade92a
13. Rossomme S, Lorentini S, Vynckier S, et al. Correction of the measured current of a small-gap plane-parallel ionization chamber in proton beams in the presence of charge multiplication. *Z Med Phys*. 2021;31:192-202. doi:10.1016/j.zemedi.2021.01.008
14. Zankowski C, Podgorsak EB. Determination of saturation charge and collection efficiency for ionization chambers in continuous beams. *Med Phys*. 1998;25:908-915. doi:10.1118/1.598269
15. Burns DT, McEwen MR. Ion recombination corrections for the NACP parallel-plate chamber in a pulsed electron beam. *Phys Med Bio*. 1998;43:2033-2045. doi:10.1088/0031-9155/43/8/003
16. Mirandola A, Maestri D, Magro G, et al. Determination of ion recombination and polarity effects for the PTW advanced Markus ionization chamber in synchrotron based scanned proton and carbon ion beams. *Physica Medica*. 2022;96:149-156. doi:10.1016/j.ejmp.2022.03.007
17. Tan HQ, Lew KS, Koh CWY, et al. The effect of spill change on reliable absolute dosimetry in a synchrotron proton spot scanning system. *Med Phys*. 2023;50:4067-4078. doi:10.1002/mp.16531
18. Yeap PL, Lew KS, Koh WYC, et al. Proton Beam Range and Charge Verification Using Multilayer Faraday Collector. *Technol Cancer Res Treat*. 2024;23:15330338241262610.
19. PTW Freiburg PTW freiburg GmbH 2023 detectors for ionizing radiation: Online catalog
20. Weinhous MS, Meli JA. Determining Pion, the correction factor for recombination losses in an ionization chamber. *Med Phys*. 1984;11:846-849. doi:10.1118/1.595574
21. Jeffery PN, Boag JW, Johns HE. Electron avalanche amplification in X-ray imaging devices. *Phys Med Biol*. 1974;19:593-604. doi:10.1088/0031-9155/19/5/001
22. DeBlois F, Zankowski C, Podgorsak EB. Saturation current and collection efficiency for ionization chambers in pulsed beams. *Med Phys*. 2000;27:1146-1155. doi:10.1118/1.598992
23. Palmans H, Thomas RAS, Duane S, Sterpin E, Vynckier S. Ion recombination for ionization chamber dosimetry in a helical tomotherapy unit. *Medi Phys*. 2010;37:2876-2889. doi:10.1118/1.3427411
24. Noda K, Furukawa T, Shibuya S, et al. Source of spill ripple in the RF-KO slow-extraction method with FM and AM. *Nucl Instrum Methods Phys Res A*. 2002;492:241-252.
25. Burguete J, García-Cardosa M, Antolín E, Aguilar B, Azcona JD. Stochastic model for predicting the temporal structure of the plan delivery in a synchrotron-based pencil beam scanning proton therapy system. *Radiat Phys Chem* 2025;226:112276.
26. Tan HQi, Lew KS, Koh CWY, et al. Implementing dispersion measurement as part of scanning proton therapy commissioning and quality assurance. *Phys Med Biol*. 2023;68:225001. doi:10.1088/1361-6560/ad0536

27. CE DA, M-T N, Rapport BIPM-1986/12: Comparisons between IRD and BIPM exposure and air-kerma standards for cobalt-60 gamma rays. Rapport BIPM-1986/12.
28. Boutillon M. Volume recombination parameter in ionization chambers. *Phys Med Biol*. 1998;43:2061-2072. doi:10.1088/0031-9155/43/8/005

How to cite this article: Gan JK, Lew KS, Chua CGA, et al. Ion recombination correction in reference dosimetry for pencil beam scanned proton beams. *Med Phys*. 2026;53:e70466. https://doi.org/10.1002/mp.70466